Applied Catalysis B: Environmental 180 (2016) 44–52

Contents lists available at ScienceDirect

Applied Catalysis B: Environmental

journal homepage: www.elsevier.com/locate/apcatb

Degradation of 1,4-dioxane from industrial wastewater by solar photocatalysis using immobilized NF-TiO_2 composite with monodisperse TiO_2 nanoparticles

Helen Barndõk[a], Daphne Hermosilla[a,*], Changseok Han[b], Dionysios D. Dionysiou[b], Carlos Negro[a], Ángeles Blanco[a]

[a] Department of Chemical Engineering, Universidad Complutense de Madrid, Avda. Complutense, s/n, 28040 Madrid, Spain.
[b] Environmental Engineering and Science Program, Department of Biomedical, Chemical and Environmental Engineering (DBCEE), University of Cincinnati, Cincinnati, OH, USA.

ARTICLE INFO

Article history:
Received 24 February 2015
Received in revised form 24 May 2015
Accepted 11 June 2015
Available online 16 June 2015

Keywords:
NF-TiO_2
Monodisperse titania
Immobilized catalyst
Photocatalysis
1,4-Dioxane

ABSTRACT

The degradation of 1,4-dioxane was accomplished by solar photocatalysis using an immobilized nitrogen and fluorine co-doped titanium dioxide (NF-TiO_2) composite with monodisperse TiO_2 nanoparticles. The effect of different wastewater matrices was studied, and the treatment of an industrial effluent contaminated with 1,4-dioxane was carried out. Compared to the degradation rate in a synthetic solution ($k_{dioxane} = 0.34 \pm 0.02\ h^{-1}$), 1,4-dioxane removal decreased in the industrial wastewater ($k_{dioxane} = 0.27 \pm 0.01\ h^{-1}$) due to the presence of inorganic constituents, whereas, the increase of the effluent pH to 6.9 produced only a slight decrease of the photocatalytic efficiency ($k_{dioxane} = 0.31 \pm 0.01\ h^{-1}$). In the photocatalytic treatment of the industrial effluent, almost complete degradation of 1,4-dioxane ($\leq$100%) was achieved along with 65% and 50% removal of COD and TOC, respectively. Moreover, remarkably similar results (about 50% of COD removal in 6 h) were achieved using both the immobilized lab-made catalyst and the commercial P25-TiO_2. In the chromatographic study of metabolites, ethylene glycol diformate, ethylene glycol monoformate, and formic acid were identified as major reaction intermediates, and thereby, the main reaction pathways have been proposed. The progressive decrease of the partial oxidation efficiency down to about 0.2 and the moderate increase of the mean oxidation state of carbon in the solution (up to +0.5) indicate that a complete mineralization of the contamination from the current industrial effluent could be feasible using this supported catalyst.

1. Introduction

Continuous xenobiotic contamination of water by 1,4-dioxane is an emerging problem due to its adverse impact on human health. This widely used industrial solvent and common by-product from several chemical processes is known to induce kidney failure and liver damage. Furthermore, since animal studies reported its tumour promoter properties, it has been classified as a probable human carcinogen (Group 2B) [1–5].

Although several modified biological processes have attained the biodegradation of 1,4-dioxane at low concentrations and long residence times [6–8], 1,4-dioxane is easily found in the downstream of industrial effluents, which indicate the inefficiency of traditional secondary treatments for complete removal of this compound [5,9,10].

As it is well known, advanced oxidation processes (AOPs) are able to effectively decontaminate effluent streams containing biorefractory organic substances [11–14]. In particular, titanium dioxide (TiO_2)-based photocatalysis offers several potential advantages with respect to typical Fenton-based AOPs such as milder reaction conditions, more flexibility in operation variables, and no waste/sludge production [15]. TiO_2 is suitable for water treatment purposes since it is an inert and rather inexpensive material [16,17]. Moreover, solar light is an economical alternative for the UV radiation, as the expense of electricity constitutes one of the major drawbacks for the implementation of photocatalytic water treatment and, thus, more and more research is focusing on sunlight-driven photo-reactors [18–21].

* Corresponding author. Fax: +34 91 394 4243.
E-mail addresses: hbarndok@quim.ucm.es (H. Barndõk), dhermosilla@quim.ucm.es (D. Hermosilla), hanck@mail.uc.edu (C. Han), dionysios.d.dionysiou@uc.edu (D.D. Dionysiou), cnegro@quim.ucm.es (C. Negro), ablanco@quim.ucm.es (Á. Blanco).

http://dx.doi.org/10.1016/j.apcatb.2015.06.015
0926-3373/

The traditional TiO_2-based photocatalysis in slurry suspension [13,22–28] requires a subsequent filtration step to remove TiO_2 particles from water, increasing the treatment cost. The immobilization of the photocatalyst is of great interest to enhance the process engineering since it allows a straight-forward separation and recovery of the catalyst from the process stream [13,26,29–31]. Immobilization, on the other hand, could restrict the reactant mass transfer [13,26], which is the main obstacle to overcome in the ongoing research regarding the industrial viability of supported photocatalysts.

Several methods have been reported to enhance the photocatalytic properties of titania, including doping, dye-sensitization, noble metal deposition, and coupled semiconductors [16,32–36]. For instance, the addition of gold nanoparticles on the surface of TiO_2 powder has been reported to increase the photocatalytic degradation of 1,4-dioxane in a slurry [25], yielding removals close to 60% in 4 h. With regard to immobilized TiO_2, however, very few studies deal with the photodegradation of 1,4-dioxane on modified TiO_2. Nakajima et al. [37] reported a 30% removal of the compound in 4 h of UV radiation using TiO_2–$Cs_{2.5}H_{0.5}PW_{12}O_{40}$ hybrid films.

Among the various approaches, non-metal doping is an advantageous technique to improve the photoactivation of TiO_2 at a broader range of solar spectrum compared to metal-doped TiO_2, since the possible toxicity emission associated to metal leaching diminishes its potential for environmental applications. Successful water remediation was obtained by nitrogen and fluorine doped titania (NF-TiO_2) [38], and the immobilization of this catalyst resulted in active and mechanically stable photocatalytic films [31]. Moreover, the optical and physicochemical properties of the film for NF-TiO_2 photocatalysis were improved by adding P25-TiO_2 nanoparticles into the NF-TiO_2 sol–gel [39]. In a recent study [40], the incorporation of lab-made monodisperse titania nanoparticles [29] layer-by-layer on NF-TiO_2, instead of the direct addition of P25-TiO_2, further improved the catalyst, resulting in an effective degradation of various wastewater contaminants. However, the performance of immobilized NF-TiO_2 composite with monodisperse TiO_2 (NF-TiO_2-monodisp.TiO_2) has not been tested on heavily loaded industrial effluents containing contaminants such as 1,4-dioxane.

In fact, photocatalytic degradation studies of 1,4 dioxane have all been performed in synthetic solutions with ultrapure water [13,22–28,37,41,42], whereas, usually very low initial concentrations are treated. Thus, although the substantial concentrations of salts and alkalinity often present in wastewaters could abate the effectiveness of the photocatalysis [24,43,44], their effect on the removal of 1,4-dioxane from heavily loaded industrial effluents by photocatalysis has not been assessed yet.

Therefore, in this study, the treatment of wastewaters containing 1,4-dioxane by solar photocatalysis using an immobilized NF-TiO_2-monodisp.TiO_2 as photocatalyst was studied. The effect of various wastewater matrices on the removal of 1,4-dioxane was studied and a treatment of an industrial wastewater contaminated with 1,4-dioxane was carried out. Comparative experiments were also conducted with commercial P25-TiO_2 in suspension. Furthermore, the main reaction pathways were proposed by identifying the major reaction intermediates of solar light-induced NF-TiO_2 photocatalysis of 1,4-dioxane.

2. Materials and methods

2.1. Wastewater samples

Industrial wastewater contaminated by 1,4-dioxane outflowing a biological treatment was supplied by a chemical factory. A synthetic solution (140 mg L^{-1}) of 1,4-dioxane (Sigma–Aldrich® Chemie GmbH, Steinheim, Germany) was also prepared with ultrapure deionized water. The initial pH of the synthetic solution was 5.7. Since the industrial wastewater under concern had a relatively high bicarbonate alkalinity and concentration of inorganic salts (Table 1) as well as a pH higher than the one of a synthetic solution, the effect of these characteristics on the degradation of 1,4-dioxane by solar light-induced NF-TiO_2 photocatalysis was investigated. Therefore, the experiments were run at pH 6.9, analogous to the industrial effluent, achieved either by adding sodium hydroxide (Panreac S.A., Barcelona, Spain) or by simulating the inorganic content of the industrial wastewater with calcium chloride, magnesium heptahydrate, sodium bicarbonate, and sulphuric acid, supplied by Panreac S.A. (Barcelona, Spain).

Table 1
Main characteristics of the industrial effluent.

Characteristic	Value
1,4-Dioxane, mg$C_4H_8O_2$ L^{-1}	135–140
COD, mgO_2 L^{-1}	245–255
TOC, mgC L^{-1}	76–80
pH	6.9
Conductivity, mS cm^{-1}	2.44
Alkalinity, mg$CaCO_3$ L^{-1}	270–280
Chlorides, mgCl^- L^{-1}	500–550
Sulphates, mgSO_4^{2-} L^{-1}	240–260

2.2. Photocatalysts

Aeroxide® P25-TiO_2 photocatalyst with a specific surface area (BET) of 50 ± 15 m^2 g^{-1}, pore volume of 0.25 m^3 g^{-1} and an average primary particle size of 21 nm was supplied by Evonik (Essen, Germany). The composite NF-TiO_2-monodisp.TiO_2 films were prepared by a modified method reported by Barndõk et al. [40]. Briefly, two different TiO_2 solutions were alternately deposited on a borosilicate substrate by dip-coating using a so-called layer-by-layer method (6 layers in total). The NF-TiO_2 sol was prepared using a modified sol–gel method similar to that reported by Pelaez et al. [31], and the solution of monodisperse anatase titania with a particle size of 50 nm was synthesized by a method described by Han et al. [29]. Shortly, the NF-TiO_2 sol was made up of fluorosurfactant Zonyl FS 300 (Fluka, Steinheim, Germany), isopropyl alcohol (Panreac S.A., Barcelona, Spain), glacial acetic acid (Panreac, S.A., Barcelona, Spain), ethlyenediamine (Fluka, Steinheim, Germany), and titanium tetraisopropoxide (TTIP; Sigma–Aldrich® Chemie GmbH, Steinheim, Germany). Monodisperse anatase titania sol was prepared by adding TTIP to methanol (Panreac S.A., Barcelona, Spain) in the presence of $CaCl_2$. Each layer was prepared using a home dip-coating apparatus with an average dipping-withdrawal speed of 12.5 cm min^{-1}, whereas, after each coating, the film was dried with an infrared lamp for 20 min and subsequently calcined at 400 °C during 30 min and cooled down naturally.

2.3. Characterization of the films

The crystallographic structure of the synthesized TiO_2 films was determined by X-ray diffractometry (XRD) using a Grazing incident method in a Philips X'pert pro MRD instrument with a parabolic mirror in the primary optic and a parallel plate collimator with a secondary monochromator in the secondary optic. The radiation used was Cu K–α (λ = 1.54 Å). The Brunauer–Emmett–Teller (BET) surface area, pore volume, porosity, Barret–Joyner–Halenda (BJH) pore size and distribution were determined by ASAP 2020 physisorption analyzer (Micromeritics). Before the analysis, the samples were purged with N_2 for 2 h at 150 °C. The morphology of the catalytic film was characterized with a JEOL 7600F scanning electron microscope (SEM). For SEM analysis, the films were coated

with carbon. To obtain detail information of the crystal size and structure at nanoscale, transmission electron microscopy (TEM) was carried out with a JEM 3000F microscope (point resolution of 0.17 nm). For TEM analysis, the samples were ultrasonically dispersed in butanol (99.5%, Panreac, Spain) and then deposited on a copper grid covered with a holey carbon film. For BET, XRD and TEM analyses, powdered samples were obtained by scraping the TiO_2 films.

2.4. Dark adsorption experiments

20 mL of 1,4-dioxane solution of various initial concentrations (25, 50, 100, 150 and 200 mg L^{-1}) were kept for 24 h in contact with two immobilized NF-TiO_2-monodisp.TiO_2 films with a total coated area of 25 cm^2 on the substrates inside sealed plastic vessels under dark conditions. Blank control reactors containing 1,4-dioxane without the photocatalyst were also left in the dark for 24 h. The experiments were carried out in triplicates, and TOC was used as an analytical parameter to assess the change in the concentration of 1,4-dioxane in the solution.

2.5. Photocatalytic experiments

The photocatalytic degradation of 1,4-dioxane was carried out in a borosilicate glass vessel reactor (i.d. 11.5 cm) containing 50 mL of actual or synthetic wastewater (approx. 0.50 cm of aqueous irradiated layer) and 5 photocatalytic films with a total coated area of 75 cm^2. The quartz cover of the reactor was sealed with parafilm and a fan was used to cool the air and prevent evaporation. The solution was irradiated with a Solar Simulator supplied by Newport (Irvine, USA) equipped with a Xe lamp (1000 W m^{-2}) and a correction filter (ASTM E490-73a) to obtain the solar spectrum under ideal conditions. The total power radiated in the visible and UV region was 106.5 W (51.7% and 48.3%, respectively). Major emission bands (>3%) were located at 578.0 nm (17.4%); 546.1 nm (16.0%); 435.8 nm (10.9%); 404.5 nm (7.5%); 366.0 nm (6.3%); 334.1 nm (4.4%); 313.0 nm (3.9%); 302.5 nm (3.7%); 296.7 nm (3.6%); 289.4 nm (3.2%); 280.4 nm (3.0%); and 253.7 nm (3.6%). The light intensity on the illuminated liquid surface was 80 mW cm^{-2} within 315–400 nm at the mid-surface of the Xe lamp, measured with a radiant power meter RM21 (Dr. Göbel UV-elektronik GmbH, Ettlingen, Germany). The experiments were carried out in triplicates.

When the experiments were conducted using the P25-TiO_2 in suspension instead of immobilized films, a loading of 1.24 g L^{-1} of photocatalyst was chosen, corresponding to the available specific catalytic surface that was equal to the one available using immobilized catalysts, taking into account the BET surface area of both photocatalysts.

2.6. Analytical methods

All the analyses were performed according to the standard methods for the examination of water and wastewater [45]. Chemical oxygen demand (COD) was measured by the colorimetric method at 600 nm using an Aquamate-spectrophotometer (Thermos Scientific AQA 091801, Waltham, USA). Total organic carbon (TOC) was measured using a TOC/TN analyzer multi N/C® 3100 (Analytik Jena AG, Jena, Germany) with catalytic oxidation on cerium oxide at 850 °C. Conductivity was measured with a non ionic-selective conductivity probe GLP 31 (Crison, S.A., Barcelona, Spain). The pH was measured using a model GLP 21 pH-meter (Crison, S.A., Barcelona, Spain) and alkalinity was measured by titration with sulphuric acid 0.1N using a pH electrode connected to an automatic titrator Compact I (Crison, S.A., Barcelona, Spain). Sulphate content was determined by turbidimetric method and chloride concentration was measured colorimetrically by Spectroquant® Chloride Test (Merck KGaA, Darmstadt, Germany).

1,4-Dioxane and its metabolites, ethylene glycol diformate (EGDF), and ethylene glycol monoformate (EGMF) were identified and quantified by an Agilent 6890N gas chromatograph (GC, Palo Alto, CA) equipped with a quadrupole mass spectrometer (MS) Agilent 5975B. To extract these two volatile compounds from the water samples, an internal standard (5 mg L^{-1} of octanol) and 1.4 g of ammonium sulphate were added to 10 mL of sample, and the solution was extracted threefold with dichloromethane (40:10:10 mL). The organic fraction was dried on anhydrous sodium sulphate and concentrated to 1 mL under nitrogen flux in a Kuderna–Danish apparatus (Sigma, St. Louis, MO) and analysed by GC–MS as follows. Samples (3 μL) were injected in split mode (30:1), and volatiles were separated using a fused silica capillary column (HP-INNOWAX) (30 × 0.25 mm i.d. and 0.25 μm film thickness), supplied by Agilent (Madrid, Spain). The pressure of the GC-grade He carrier gas was 7.7 psi with a linear velocity of 1.0 mL min^{-1}; the initial oven temperature was 45 °C, first increased at 3 °C min^{-1}–100 °C, held for 1 min, and then heated at 15 °C min^{-1}–270 °C, and held at this temperature for an additional 5 min. The injection temperature was 230 °C. Detection was carried out by electron ionization (EI) mode (70 eV), interphase detection temperature was 290 °C (MS source at 230 °C and MS quad at 150 °C) and scanning mass was ranged between 35 and 400 amu. Quantitative determinations were carried out by the internal standard method, using peak areas obtained from selected ion monitoring (88, 1,4-dioxane; 60, EGDF/EGMF; 45, octanol) and calibrations made with pure reference compounds analyzed under the same conditions.

1,4-Dioxane was also quantified together with ethylene glycol as its possible degradation product, using gas–liquid chromatography (GLC) on a 7980A instrument (Agilent Technologies Inc., Palo Alto, CA) equipped with a flame ionization detector. The temperatures of the injector and detector were 310 °C and 280 °C, respectively. Samples (2 μL) were injected using the pulsed-split mode (split ratio 5:1) and analyzed in a TRB-FFAP (Teknokroma, Sant Cugat del Vallès, Spain) fused silica column (30 m × 0.25 mm internal diameter × 0.25 μm film thickness) with He (43 psi) as carrier gas and the following temperature programm: 80 °C–240 °C after 9 min initial hold and at a 15 °C min^{-1} ramp rate. Peaks were identified according to the relative retention times of commercial standards. Quantification was performed according to peak area, corrected with the response factors calculated for each compound using 1-butanol (250 ppm) as internal standard, and the software GC-ChemStation Rev.B.04.02 (96) from Agilent.

Oxalic, acetic, formic, glycolic, and methoxyacetic acids were identified and quantified by ion chromatography (IC) using a 940 Professional IC Vario instrument (Metrohm, Herisau, Switzerland) equipped with a conductivity detector. An isocratic gradient of Na_2CO_3 (3.6 mM) was used as eluent, keeping an eluent flow at 0.7 mL min^{-1}. The injection loop was 50 mL. Analysis was done in an ionic resin column Metrosep A Supp 7 with a guard column Metrosep A Supp 4/5 Guard.

2.7. Determination of the mean oxidation state of carbon and the partial oxidation efficiency

The mean oxidation state of carbon (MOSC) for a single organic molecule was calculated using Eq. (1) [46]:

$$\mathrm{MOSC}_{\mathrm{compound}} = \frac{\sum_{i=n}^{n} \mathrm{OSC}_i}{n} \quad (1)$$

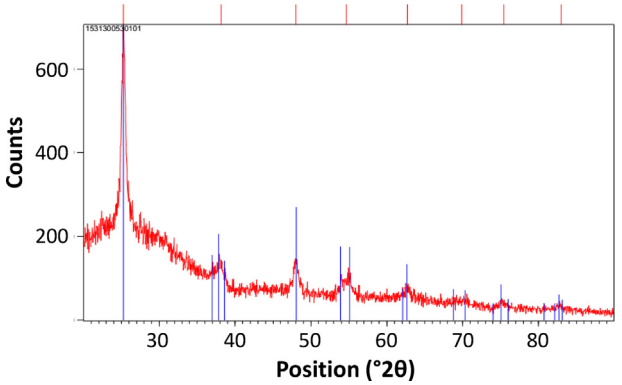

Fig. 1. XRD pattern of NF-TiO_2-monodisp.TiO_2 catalytic film.

where n is the number of carbon (C) atoms and OSC_i is the oxidation state of the ith C atom in the molecule. The determination of OSC_i is illustratively described by Ashenhurst [47].

The MOSC of wastewater was calculated from the values of TOC and COD, using Eq. (2) [46,48–50]:

$$MOSC_{wastewater} = 4 - 1.5\frac{COD}{TOC} \quad (2)$$

where COD and TOC are given in $mgO_2\ L^{-1}$.

Partial oxidation efficiency ($\mu_{CODpartox}$) was calculated by Eq. (3), where the COD of partial oxidation (COD_{partox}) was defined by Eq. (4) [48,49]:

$$\mu_{COD_{partox}} = \frac{COD_{partox}}{COD_0 - COD} \quad (3)$$

$$COD_{partox} = \frac{COD_0 \times TOC}{TOC_0} - COD \quad (4)$$

3. Results and discussion

3.1. Structural characteristics of the composite films

According to the XRD pattern of the prepared films (Fig. 1), all peaks corresponding to anatase phase at $2\theta = 25.3$, 38.0, 48.1, 54.6, 62.6, 70.5, 75.2 and 82.9, were detected by XRD analysis (JCPDF card no 00-021-1272). This indicates that anatase, the most active phase among TiO_2 phases, was synthesized with this method. Dopant-related crystal phases were not observed since the amount of N and F does not produce significant changes in the TiO_2 structure [31]. Based on the rough estimation obtained from XRD data, the crystalline size was calculated to be 8.62 nm (Table 2).A defined crystalline interconnected network can be observed from TEM images (Fig. 2), whereas, the lattice spacing of 0.352 nm, corresponding to the 1 0 1 plane of TiO_2, is well observed by the higher magnification, providing evidence on high crystallinity. According to the TEM images, there were two different size groups of particles, one with the size around 20 nm and the other one smaller than 10 nm since two different methods were used to prepare these catalyst films. With regard to monodisperse particles, it is not easy to observe their unique structure with TEM analysis because they are actually aggregates of smaller nanosized particles. The discrepancy between the crystallite sizes obtained from BET and XRD data (the degree of agglomeration, D_{BET}/D_{XRD}) indicates that the titania particles were quite highly aggregated. Considering the SEM analysis (Fig. 3), the films had a rough and porous surface quite similar to the previous findings [40]. According to the porosimetry analysis, the immobilized catalyst had a relatively moderate BET surface of $69.5\ m^2\ g^{-1}$ and porosity of 33.6%. All the main physicochemical properties are listed in Table 2.

Table 2
Physicochemical properties of NF-TiO_2-monodisp.TiO_2.

Characteristic	Value
Crystal phase	Anatase
Crystal size (D_{XRD})[a](nm)	8.62
$D_{(101)}$[b](nm)	0.352
BET surface, $m^2\ g^{-1}$	69.5
Crystal size (D_{BET})[c](nm)	22.1
Pore volume, $cm^3\ g^{-1}$	0.133
Porosity[d], %	33.6
Agglomeration (D_{BET}/D_{XRD})	2.57

[a] Based on XRD, using Scherrer equation: $D = 0.9\lambda/(B \times \cos\theta)$; B = full width at half maximum (FWHM) of the highest peak, $\lambda = 0.154$ nm.
[b] Based on Bragg's Law: $D = \lambda/(2 \times \sin\theta)$.
[c] Obtained from BET, using $D = 6000/(\rho_{anatase} \times S_{BET})$; $\rho_{anatase} = 3.9\ g^3$ cm.
[d] Based on pore volume and $\rho_{anatase}$.

Table 3
First order kinetic constants of 1,4-dioxane degradation and the linear removal rates of TOC in the solar photocatalytic treatment of 1,4-dioxane using NF-TiO_2-monodisperse TiO_2 films under different wastewater conditions.

	$k_{dioxane}$ (1st order)	k_{TOC} (linear)
Wastewater matrix	h^{-1}	$mg\ L^{-1}\ h^{-1}$
pH 5.7 (as it is)	0.34 ± 0.02	5.65 ± 0.10
pH 6.9 (+NaOH)	0.31 ± 0.01	5.62 ± 0.34
Simulated salt content	0.26 ± 0.02	4.70 ± 0.36
Industrial effluent	0.27 ± 0.01	4.16 ± 0.34

3.2. Dark adsorption

No significant adsorption of 1,4-dioxane on the supported catalyst was found during the experiments under dark conditions at different initial concentrations. The different solution pH (5.7 and 6.9) and the presence of inorganic salt content, simulating the industrial effluent, did not affect the adsorption of 1,4-dioxane either. The differences in final TOC compared with blank experiments without NF-TiO_2-monodisp.TiO_2 catalyst were statistically insignificant ($p > 0.05$) in all wastewater matrices.

3.3. Photocatalytic degradation

3.3.1. Kinetics of 1,4-dioxane degradation in different wastewater matrices

The photocatalytic treatment of 1,4-dioxane in various wastewater matrices resulted in the linear removal of TOC in time, whereas, 1,4-dioxane removal was concentration dependent, decreasing in time (Table 3). First order kinetic models for 1,4-dioxane degradation in various wastewater matrices (Fig. 4) and the corresponding kinetic constants ($k_{dioxane}$, Table 3) indicate that 1,4-dioxane removal diminished in the industrial wastewater compared to synthetic water. The degradation rate in terms of the half-life of 1,4-dioxane was in the following decreasing order for different wastewater conditions: pH 5.7 ($t_{1/2} = 124$ min) > pH 6.9 ($t_{1/2} = 134$ min) > pH 6.9, industrial effluent ($t_{1/2} = 156$ min) > pH 6.9, simulated salt content ($t_{1/2} = 161$ min). However, the difference between the overall 1,4-dioxane removals at pH 5.7 and 6.9 (90% and 88%, respectively) were insignificant, which implies that the decrease in photocatalytic degradation rates was caused by the presence of inorganic constituents.

In fact, when considering the mineralization of organics in terms of TOC removal (k_{TOC}, Table 3), no significant differences were found, neither between the experiments at pH 5.7 and pH 6.9, nor between the experiments comparing industrial effluent and synthetic water with simulated salt content. The degradation of TOC per unit area of the coated catalyst surface (Fig. 5) was about $3.4\ \mu gC\ cm^{-2}\ h^{-1}$ in synthetic wastewaters at both pH 5.7 and pH 6.9; whereas, about $2.8\ \mu gC\ cm^{-2}\ h^{-1}$ was degraded in both the

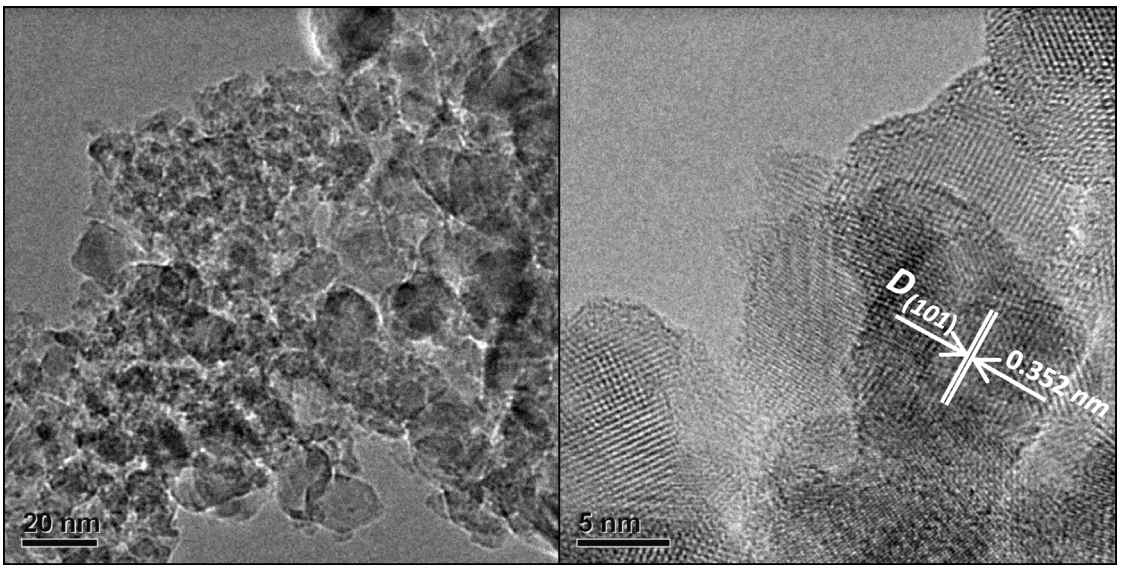

Fig. 2. TEM image of NF-TiO_2-monodisp.TiO_2 catalytic film.

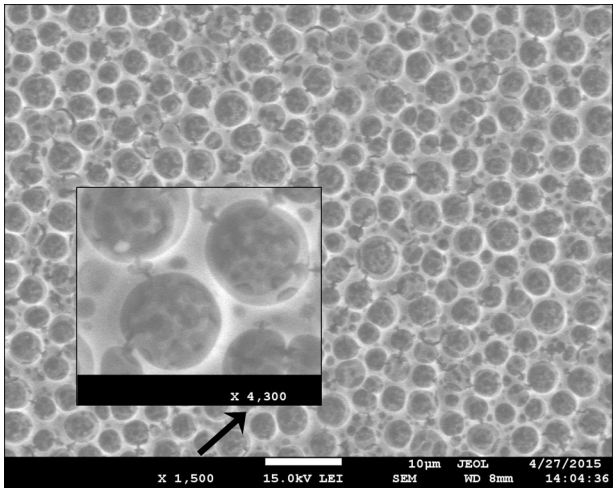

Fig. 3. SEM image of NF-TiO_2-monodisp.TiO_2 catalytic film.

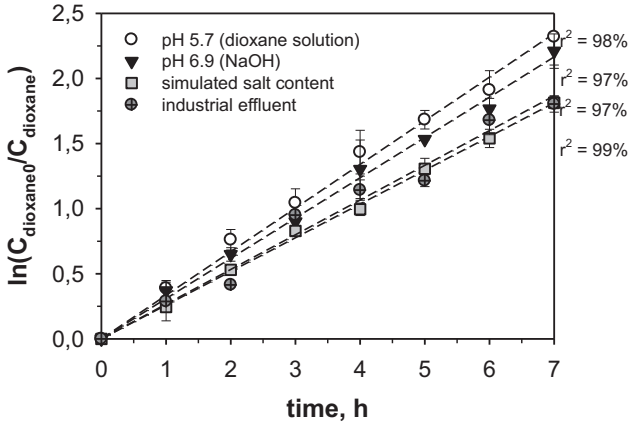

Fig. 4. First order kinetic model for the solar photocatalytic degradation of 1,4-dioxane on immobilized NF-TiO_2-monodisp.TiO_2 under different wastewater conditions.

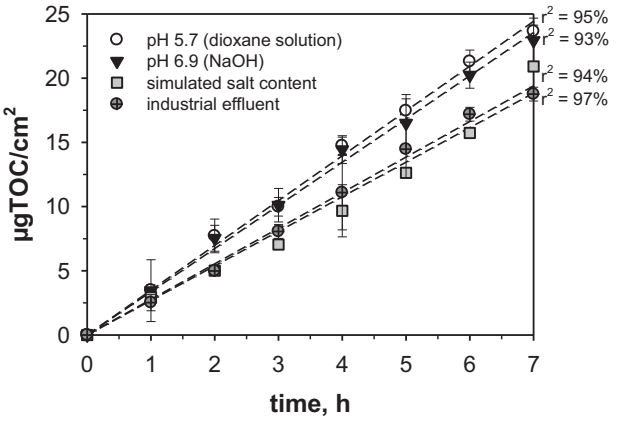

Fig. 5. Decomposition amount of TOC per unit of film area in the solar photocatalytic degradation of 1,4-dioxane on immobilized NF-TiO_2-monodisp.TiO_2 under different wastewater conditions.

industrial effluent and synthetic water with previously added salt content.

Since the surface of NF-TiO_2 is negatively charged at pH above ≈6 [38] and the molecule of 1,4-dioxane acts as an electron donor by its definition as a Lewis base [51], an inhibition in the photocatalytic degradation of 1,4-dioxane at pH above 6 could be expected due to the repulsive electrostatic forces between the catalyst and the contaminant. However, the results of this study show that this effect is not pronounced in a great extent at the pH of the real industrial effluent (pH 6.9).

On the other hand, when the inorganic content was present, either initially in the industrial effluent or in a form of added salts, the photocatalytic degradation of both 1,4-dioxane and TOC decreased (Figs. 5 and 6). The negative effect of inorganic anions on the efficiency of photocatalytic oxidation has been attributed to various mechanisms, such as •OH radical and "hole" scavenging [43], and competitive adsorption [44]. Although the adsorption of 1,4-dioxane on the surface of NF-TiO_2-monodisperse TiO_2 was found to be negligible for all the wastewater matrices (Section 3.2.), there is always a concentration gradient through a molecular transfer toward the catalyst surface because the photocatalytic degradation is expected to occur at the liquid–solid interface [52,53]. Therefore, the concentration and adsorption of inorganic

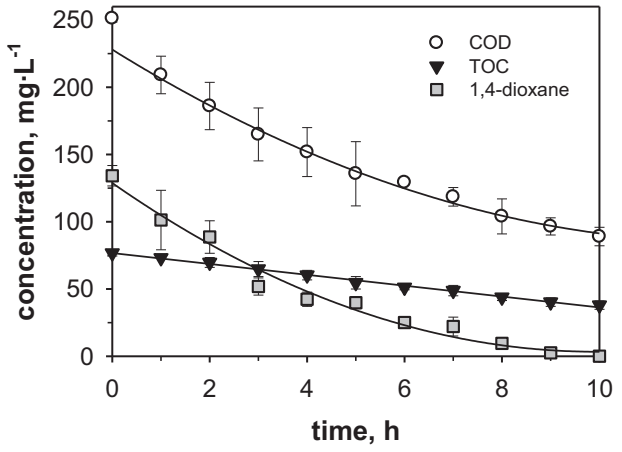

Fig. 6. The evolution of the concentrations of 1,4-dioxane, COD and TOC in the treatment of an industrial effluent containing 1,4-dioxane by solar photocatalysis using NF-TiO_2-monodisp.TiO_2 films.

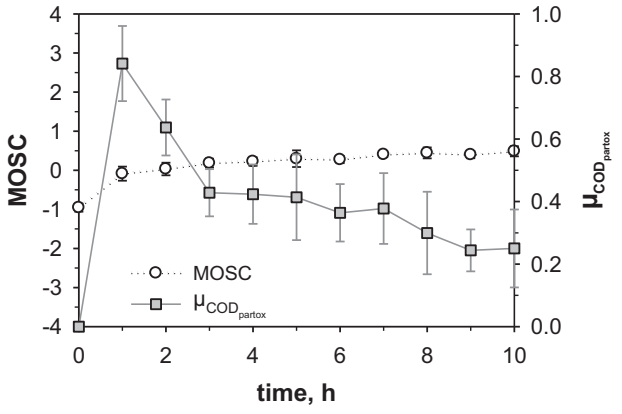

Fig. 7. The evolution of the mean oxidation state of carbon (MOSC) and the partial oxidation efficiency ($\mu_{CODpartox}$) in the treatment of an industrial effluent containing 1,4-dioxane by solar photocatalysis using NF-TiO_2-monodisp.TiO_2 films.

anions on the surface of TiO_2 could result in a loss of active sites for the oxidation of organic molecules [43,44].

On the other hand, our previous research [54] and the investigation performed by Merayo et al. (2013, unpublished research) shows that the inorganic content could reduce the photocatalytic efficiency simply due to the increase of ionic strength or by modifying the solution pH. According to a previous study, neither sulphates nor chlorides affect the UV/TiO_2 oxidation of phenol, whereas, carbonates decrease its removal along with the increasing pH [54]. However, no important negative effect on the 1,4-dioxane degradation was found under the higher pH conditions of the industrial wastewater, as discussed above (Figs. 4 and 5).

3.3.2. *Photocatalytic treatment of industrial wastewater containing 1,4-dioxane*

In the photocatalytic treatment of an industrial effluent, the degradation of 1,4-dioxane (≤100%) was almost completed along with the 65% and 50% removal of COD and TOC, respectively (Fig. 6). While the concentration of TOC decreased in a linear manner, the degradation of COD followed a trend similar to that of 1,4-dioxane removal (the first order rate constant was $k_{COD} = 0.11\ h^{-1}$, $r^2 = 97\%$), which implies the accumulation and slower degradation of reaction intermediates produced during the photocatalysis.

Both the identification and quantification of the multiple reaction products by chromatographic analyses can be extremely laborious and expensive for the complex industrial wastewater.

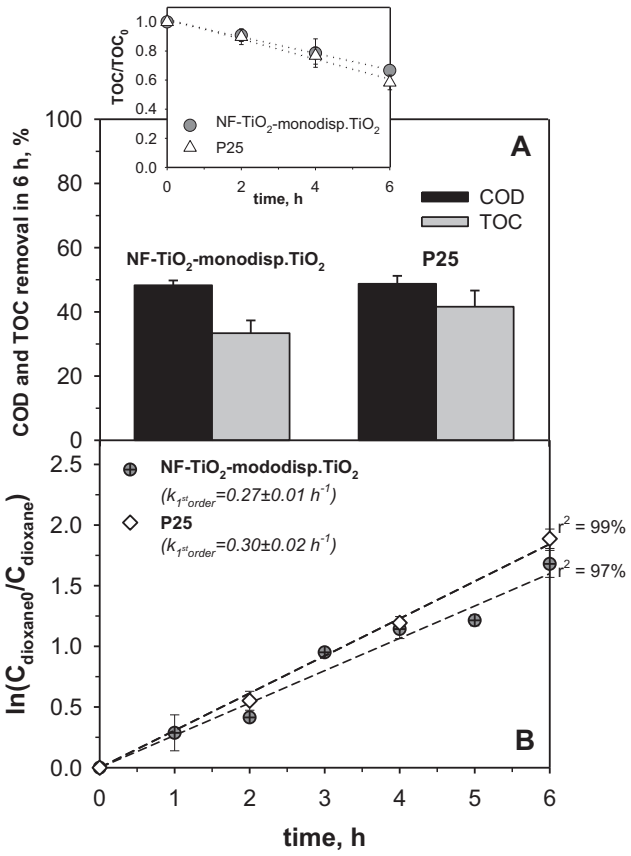

Fig. 8. Comparison of COD and TOC removals after 6 h of solar photocatalytic degradation of an industrial effluent containing 1,4-dioxane using an immobilized film of NF-TiO_2-monodisp.TiO_2 and commercial TiO_2-P25 (Aeroxide®) in suspension.

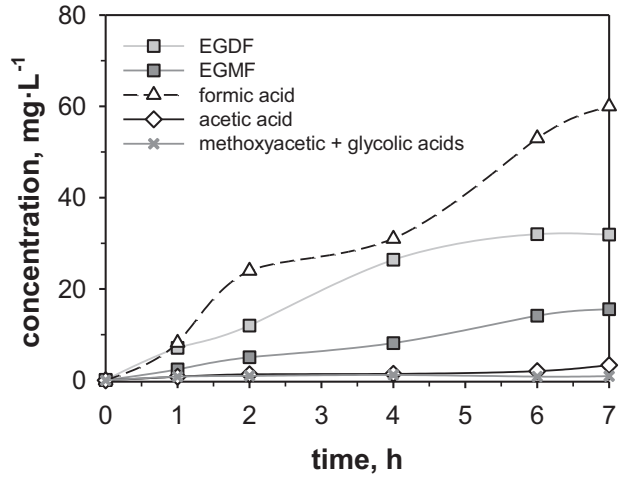

Fig. 9. Primary reaction intermediates in the photocatalytic degradation of 1,4-dioxane under solar light using immobilized NF-TiO_2-monodisp.TiO_2.

Nevertheless, the MOSC (Eqs. (1) and (2)) can be a useful parameter to understand reaction development during wastewater treatment, providing valuable information about the possible oxidative transformations [46,48–50]. MOSC can vary from −4 (e.g., CH_4) to +4 (e.g., CO_2); however, as CO_2 is released from the solution, it does no account for the solution MOSC, which is a proportional average of the molecular MOSC values of all the compounds present in the effluent. The $\mu_{CODpartox}$ (Eq. (3)) provides a better understanding of the mineralization capacity of an oxidative system, indicating

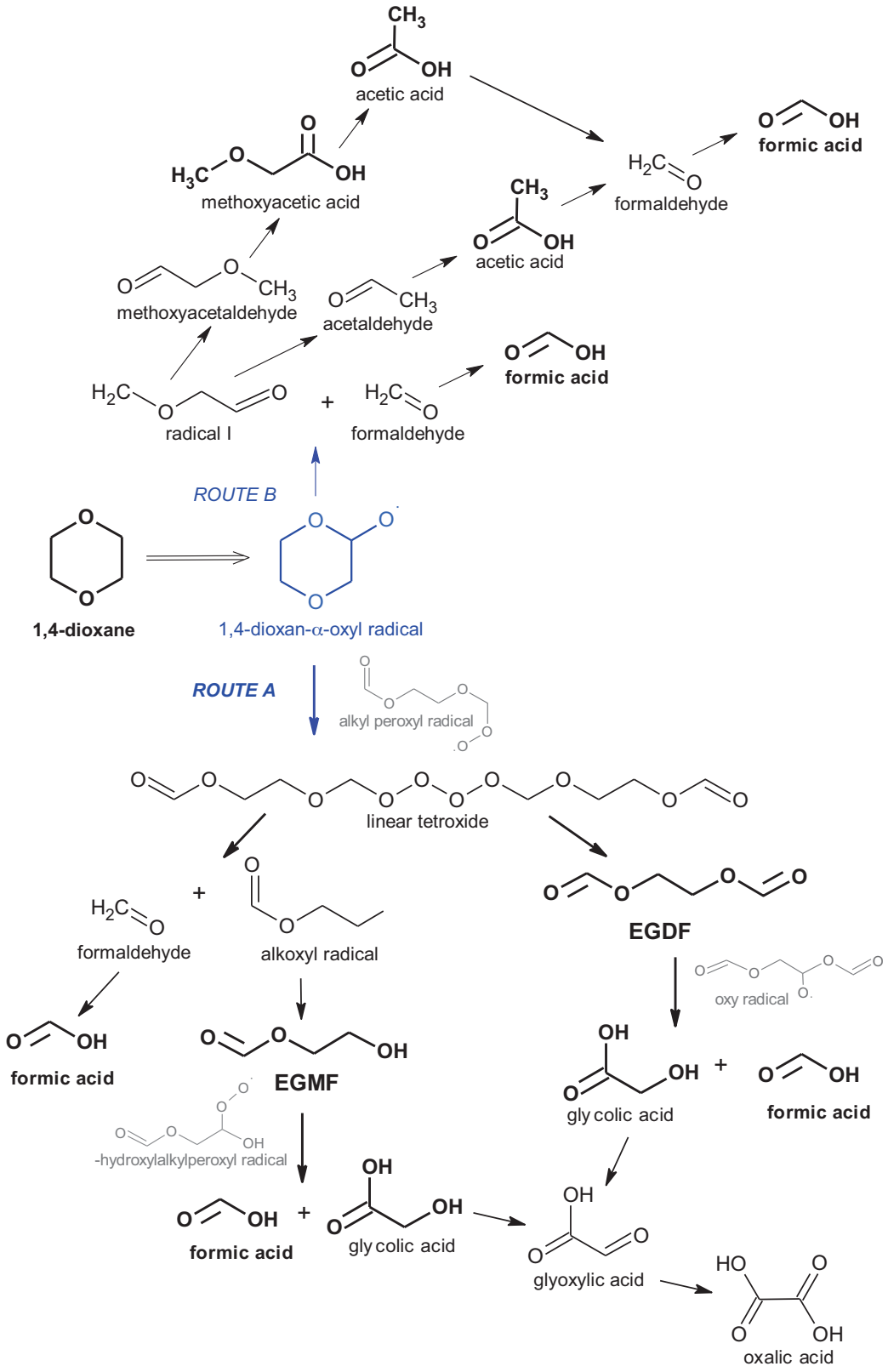

Fig. 10. Simplified schematic of the major reaction pathways proposed for 1,4-dioxane degradation

the percentage of COD decrease that does not lead to mineralization, but result in oxygenated products other than CO_2 and H_2O (COD_{partox}).

In the photocatalytic treatment of the industrial effluent using immobilized NF-TiO_2-monodisp.TiO_2, the MOSC of the wastewater increased from about −1 to 0 in the first 60 min, as 1,4-dioxane molecule ($MOSC_{dioxane} = -1$) was being oxidized; and continued to increase more slowly during the rest of the experiment, indicating an accumulation of reaction intermediates with an average MOSC of about +0.5 (Fig. 7). This is in accordance with the following chro-

matographic study (section 3.3.3) where EGDF ($MOSC_{EGDF}$ = +1) and EGMF ($MOSC_{EGMF}$ = 0) were found as major primary metabolites. Although the solution MOSC remained relatively low, the $\mu_{CODpartox}$ progressively decreased to about 0.2, as expected when organics are degraded to CO_2 and water [48,49]. Therefore, rapid mineralization of simpler carboxylic acids is suspected.

According to Nakajima et al. [37], the low decomposition of EGDF during photocatalysis is due to its poor affinity with TiO_2. In the photocatalytic treatment of waters contaminated by 1,4-dioxane, the fastest removal rates are usually reported using commercial P25-TiO_2 in suspension [24,26]. To improve the cost-effectiveness of the process, immobilization of the photocatalysts is of great interest, as the separation and recovery of the catalyst from the process stream is straight-forward [13,26,29–31]. In order to compare the performance of the immobilized NF-TiO_2-monodisp.TiO_2 catalyst with the P25-TiO_2 slurry suspension, experiments were carried out using a concentration of P25 that corresponds to the available specific catalytic surface that was equal to the one available using the immobilized catalysts, taking into account the BET surface area of both photocatalysts. These experiments, however, resulted in COD and TOC removals remarkably similar to the ones obtained by the immobilized catalyst (Fig. 8A). Namely, in the same treatment period of 6 h, 49% and 50% COD, and 34% and 40% TOC were respectively removed when using NF-TiO_2-monodisp.TiO_2 films and P25 suspension. In fact, differences were statistically insignificant ($P > 0.05$). The first order rate constant for the degradation of 1,4-dioxane was only slightly higher with P25 suspension (Fig. 8B). Obtaining results by an immobilized catalyst which are similar as those obtained by P25 in suspension is an encouraging result. Generally, the superiority of P25 catalyst is well-known and higher removals are always reported when working with slurry systems [13,26].

The slow but persistent removal of carbon in the experiments with the supported catalyst reflects that a complete mineralization of contamination from the real industrial effluent could be feasible using immobilized NF-TiO_2-monodisp.TiO_2. Total mineralization could be reached either by elongating the reaction time or, preferably, by increasing the catalyst surface. Thus, a further study on optimizing the reactor design would be of great interest. Using an immobilized catalyst would permit working without the need of an additional costly filtration step, which would greatly enhance the engineering of the process [13,26,29–31].

3.3.3. *Reaction intermediates of 1,4-dioxane photocatalytic decomposition*

In the study of decomposition routes along with the removal of 1,4-dioxane in the course of photocatalytic oxidation, various degradation products appeared (Fig. 9). EGDF, EGMF and formic acid were identified as major reaction intermediates. In lesser extent ($\leq 4.0 \pm 0.1$ mg L^{-1}), some acetic acid was produced along the process, while traces of methoxyacetic and glycolic acids were detected as mixture at concentrations below 1.16 ± 0.06 L^{-1}.

Fig. 10 presents a simplified schematic of the major reaction pathways proposed for 1,4-dioxane degradation. According to the literature, EGDF and EGMF are produced concurrently in an oxidative ring opening mechanism initiated by •OH radical, whereat 1,4-dioxan-α-oxyl radical has been suggested to be the precursor, as described in detail by [41,55]. This α-oxyl radical can be degraded either through ΔC–C splitting at the *α–C* position (route A) or through an intramolecular reaction (H abstraction from the *αí–C* position) followed by fragmentation (route B).

Considering the chromatography analysis, route A was the primary degradation pathway in which, in accordance with the literature, it is suggested that the linear tetroxide generated over alkyl peroxyl radicals decomposed either to EGDF or to alkoxyl radical that lead to EGMF and formaldehyde [41]. Formaldehyde is readily oxidized to formic acid [56], and, in addition, formic acid is also produced along with glycolic acid in the further decomposition of both EGDF and EGMF [24,41]. However, the low concentrations of glycolic acid detected and the continuous decrease of TOC measured most likely refer to its very fast subsequent mineralization over oxalic acid [41]. In addition, it is important to note that, although reported as possible route for 1,4-dioxane degradation in different AOPs [24,55,57], ethylene glycol was not detected during the experiment, showing that no hydrolysis of the EGDF and EGMF took place in this photocatalytic process.

In the alternative route B (Fig. 10), formaldehyde and, thus, formic acid are also produced along with the *C*-centered radical I, which in turn supports the higher concentrations of formic acid in the system (Fig. 9). Radical I is either reduced to methoxyacetaldehyde, which is subsequently oxidized to methoxyacetic and acetic acids, or it proceeds through β-scission yielding acetaldehyde and, consequently, acetic acid [41,55,56]. Nevertheless, taking into account the low concentrations of methoxyacetic and acetic acids, the mechanism through EGDF and EGMF formation must have been predominant. In fact, similar pathway, mainly through the formation of the EGDF concurrently with a minor route for the formation of methoxiacetic acid, was observed by FTIR monitoring in a recent study on ozone oxidation of 1,4-dioxane under acidic conditions [57].

Despite the fact that the concentration of formic acid ($MOSC_{formic}$ = +2) increased throughout the experiment, indicating its continuous production, the relatively low solution MOSC (0. . .+0.5; Fig. 7) also implied its continuous mineralization, considering its high rate constant with •OH radical (3.2×10^9 M^{-1} s^{-1} [58]). Moreover, the progressive decrease of the partial oxidation efficiency down to about 0.2 (Fig. 7) and the linear removal of TOC from the system (Fig. 6) also account for the continuous production of CO_2 and water.

4. Conclusions

Wastewaters containing 1,4-dioxane were successfully treated by solar photocatalysis using an immobilized NF-TiO_2 composite with monodisperse TiO_2 nanoparticles. Degradation of 1,4-dioxane decreased in the industrial effluent mainly due to its inorganic constituents, whereas, the change in effluent pH only produced a slight decrease in the degradation efficiency. Removal decreased for different wastewater conditions in the following order: pH 5.7 ($k = 0.34 \pm 0.02$ h^{-1}) > pH 6.9 ($k = 0.31 \pm 0.01$ h^{-1}) > industrial effluent ($k = 0.27 \pm 0.01$ h^{-1}) > simulated salt content ($k = 0.26 \pm 0.01$ h^{-1}). The mineralization was about 3.4 μgC cm^{-2} h^{-1} in synthetic waters at both pH 5.7 and pH 6.9; whereas, about 2.8 μgC cm^{-2} h^{-1} were degraded in both the industrial effluent and the solution with a simulated inorganic content.

Despite the salt content, the complete removal of 1,4-dioxane (≤100%) from the industrial wastewater was achieved along with a 65% and 50% of COD and TOC, respectively. Similar results ($P > 0.05$) were achieved by the immobilized lab-made catalyst and by the commercial P25-TiO_2. Namely, 49% and 50% COD, and 34% and 40% TOC were removed after 6 h of treatment with NF-TiO_2-monodisp. TiO_2 films and the P25 suspension, respectively.

The solar photocatalysis of 1,4-dioxane on NF-TiO_2-monodisp.TiO_2 was predominantly dependent on the slow degradation of primary intermediates, EGDF and EGMF, produced concurrently in an oxidative ring opening mechanism initiated by •OH. In addition, formic acid was continuously generated in various simultaneous degradation reactions, whereas, its steady removal from the system is also suggested alongside with the other simple carboxylic acids. Such a slow but persistent removal of

organic carbon throughout the experiment reflects that a complete mineralization of contamination from actual industrial effluents could be feasible using this supported catalyst. Immobilization, in turn, would greatly enhance the process engineering and, thus, increase the cost-effectiveness of the treatment.

Acknowledgements

The research leading to these results has received funding from the European Union's Seventh Framework Programme (FP7/2007-2013) under the grant agreement no 608490, E4Water project. The collaboration of the Gas Chromatography Service (CIB) of the Spanish National Research Council (CSIC), the Laboratory of Geochemical and Environmental Analyses of the Complutense University of Madrid and the Laboratory of CIFOR-INIA (Centro de Investigación Forestal, Instituto Nacional de Investigación y Tecnología Agraria y Alimentaria) is fully appreciated. The Archimedes Foundation (Estonia) is acknowledged for support to Helen Barndõk's Ph.D. studies.

References

[1] C.D. Adams, P.A. Scanlan, N.D. Secrist, Environ. Sci. Technol. 28 (1994) 1812–1818.
[2] J.Y. Choi, Y.J. Lee, J. Shin, J.W. Yang, J. Hazard. Mater. 179 (2010) 762–768.
[3] European Chemicals Bureau (ECB), E.U. Risk Assessment Report: 1,4-Dioxane, ISBN 92-894-1252-6, Second Priority List 21 (2002) 1-129, Office for Official Publications of the European Communities, Luxembourg, 2002.
[4] U.S Environmental Protection Agency (USEPA), Toxicological Review of 1,4-Dioxane (CAS No. 123-91-1), EPA/635/R-09/005-F, USEPA, Washington, DC, 2010.
[5] M.J. Zenker, R.C. Borden, M.A. Barlaz, Environ. Eng. Sci. 20 (2003) 423–432.
[6] T.-H. Han, J.-S. Han, M.-H. So, J.-W. Seo, C.-M. Ahn, D.H. Min, Y.S. Yoo, D.K. Cha, C.G. Kim, J. Environ. Sci. Health, Part A: Toxic/Hazard. Subst. Environ. Eng. 47 (2012) 117–129.
[7] W. Shen, H. Chen, S. Pan, Bioresour. Technol. 99 (2008) 2483–2487.
[8] M.J. Zenker, R.C. Borden, M.A. Barlaz, J. Environ. Eng. 130 (2004) 926–931.
[9] T.K.G. Mohr, Environmental Investigation and Remediation: 1,4-Dioxane and Other Solvent Stabilizers, CRC, Press, Boca Raton, 2010.
[10] J.M. Skadsen, B.L., Rice, D.J. Meyering, A case study in the City of Ann Arbor, Water Utilities, City of Anna Arbor, and Fleis & VendenBrink Engineering, Inc., 2004.
[11] I.A. Balcioglu, I.A. Alaton, M. Otker, R. Bahar, N. Bakar, M. Ikiz, J. Environ. Sci. Health Part A-Toxic/Hazard. Subst. Environ. Eng. 38 (2003) 1587–1596.
[12] V. Belgiorno, L. Rizzo, D. Fatta, C. Della Rocca, G. Lofrano, A. Nikolaou, V. Naddeo, S. Meric, Desalination 215 (2007) 166–176.
[13] H.M. Coleman, V. Vimonses, G. Leslie, R. Amal, Water Sci. Technol. 55 (2007) 301–306.
[14] C. Comninellis, A. Kapalka, S. Malato, S.A. Parsons, L. Poulios, D. Mantzavinos, J. Chem. Technol. Biotechnol. 83 (2008) 769–776.
[15] S. Perathoner, ChemH_2O, in: Leading-Edge Conference on Sustainable Water Management, 1–2 October 2013 Madrid, 2013.
[16] H. Choi, M.G. Antoniou, M. Pelaez, A.A. De la Cruz, J.A. Shoemaker, D.D. Dionysiou, Environ. Sci. Technol. 41 (2007) 7530–7535.
[17] A. Fujishima, T.N. Rao, D.A. Tryk, J. Photochem. Photobiol. C 1 (2000) 1–21.
[18] R.J. Braham, A.T. Harris, Ind. Eng. Chem. Res. 48 (2009) 8890–8905.
[19] S. Malato, P. Fernandez-Ibanez, M.I. Maldonado, J. Blanco, W. Gernjak, Catal. Today 147 (2009) 1–59.
[20] C. Singh, R. Chaudhary, K. Gandhi, J. Renew. Sustain. Energy 5 (2013).
[21] P.A. Soares, T.F.C.V. Silva, D.R. Manenti, S.M.A.G.U. Souza, R.A.R. Boaventura, V.J.P. Vilar, Environ. Sci. Pollut. Res. 21 (2014) 932–945.
[22] R.R. Hill, G.E. Jeffs, D.R. Roberts, J. Photochem. Photobiol. A 108 (1997) 55–58.
[23] S.W. Lam, M. Hermawan, H.M. Coleman, K. Fisher, R. Amal, J. Mol. Catal. A-Chem. 278 (2007) 152–159.
[24] V. Maurino, P. Calza, C. Minero, E. Pelizzetti, M. Vincenti, Chemosphere 35 (1997) 2675–2688.
[25] B.K. Min, J.E. Heo, N.K. Youn, O.S. Joo, H. Lee, J.H. Kim, H.S. Kim, Catal. Commun. 10 (2009) 712–715.
[26] T. Vescovi, H.M. Coleman, R. Amal, J. Hazard. Mater. 182 (2010) 75–79.
[27] K. Yasui, T. Isobe, S. Matsushita, A. Nakajima, J. Mater. Sci. 48 (2013) 2290–2298.
[28] N.K. Youn, J.E. Heo, O.S. Joo, H. Lee, J. Kim, B.K. Min, J. Hazard. Mater. 177 (2010) 216–221.
[29] C. Han, R. Luque, D.D. Dionysiou, Chem. Commun. 48 (2012) 1860–1862.
[30] N. Miranda-Garcia, S. Suarez, B. Sanchez, J.M. Coronado, S. Malato, M. Ignacio Maldonado, Appl. Catal. B-Environ. 103 (2011) 294–301.
[31] M. Pelaez, P. Falaras, V. Likodimos, A.G. Kontos, A.A. de la Cruz, K. O'Shea, D.D. Dionysiou, Appl. Catal. B-Environ. 99 (2010) 378–387.
[32] C. Han, V. Likodimos, J.A. Khan, M.N. Nadagouda, J. Andersen, P. Falaras, P. Rosales-Lombardi, D.D. Dionysiou, Environ. Sci. Pollut. Res. 21 (2014) 11781–11793.
[33] C. Han, M. Pelaez, V. Likodimos, A.G. Kontos, P. Falaras, K. O'Shea, D.D. Dionysiou, Appl. Catal. B-Environ. 107 (2011) 77–87.
[34] M. Pelaez, N.T. Nolan, S.C. Pillai, M.K. Seery, P. Falaras, A.G. Kontos, P.S.M. Dunlop, J.W.J. Hamilton, J.A. Byrne, K. O'shea, M.H. Entezari, D.D. Dionysiou, Appl. Catal. B-Environ. 125 (2012) 331–349.
[35] G.S. Pozan, A. Kambur, Appl. Catal. B-Environ. 129 (2013) 409–415.
[36] X. Shang, B. Li, C. Li, X. Wang, T. Zhang, S. Jiang, Dyes Pigm. 98 (2013) 358–366.
[37] A. Nakajima, S. Matsui, S. Yanagida, Y. Kameshima, K. Okada, Surf. Coat. Technol. 203 (2009) 1133–1137.
[38] M. Pelaez, A.A. de la Cruz, E. Stathatos, P. Falaras, D.D. Dionysiou, Catal. Today 144 (2009) 19–25.
[39] M. Pelaez, P. Falaras, A.G. Kontos, A.A. de la Cruz, K. O'Shea, P.S.M. Dunlop, J.A. Byrne, D.D. Dionysiou, Appl. Catal. B-Environ. 121 (2012) 30–39.
[40] H. Barndõk, M. Pelaez, C. Han, W.E. Platten III, P. campo, D. Hermosilla, A. Blanco, D.D. Dionysiou, Environ. Sci. Pollut. Res. 20 (2013) 3582–3591.
[41] M.I. Stefan, J.R. Bolton, Environ. Sci. Technol. 32 (1998) 1588–1595.
[42] S. Yamazaki, N. Yamabe, S. Nagano, A. Fukuda, J. Photochem. Photobiol. A 185 (2007) 150–155.
[43] R.A. Burns, J.C. Crittenden, D.W. Hand, V.H. Selzer, L.L. Sutter, S.R. Salman, J. Environ. Eng. 125 (1999) 77–85.
[44] H.Y. Chen, O. Zahraa, M. Bouchy, J. Photochem. Photobiol. A 108 (1997) 37–44.
[45] APHA, AWWA, W.P.C.F, Standard Methods for the Examination of Water and Wastewater, APHA, AWWA, WPCF, Washington, DC, 2005.
[46] F. Vogel, J. Harf, A. Hug, P.R. von Rohr, Water Res. 34 (2000) 2689–2702.
[47] J.A. Ashenhurst, Calculating the oxidation state of a carbon, http://www.masterorganicchemistry.com/2011/07/25/calculating-the-oxidation-state-of-a-carbon (2011), (accessed 07.01.14).
[48] M. Carbajo, F.J. Beltran, O. Gimeno, B. Acedo, F.J. Rivas, Appl. Catal. B-Environ. 74 (2007) 203–210.
[49] D. Hermosilla, M. Cortijo, C.P. Huang, Chem. Eng. J. 155 (2009) 637–646.
[50] N. Merayo, D. Hermosilla, C. Negro, A. Blanco, Chem. Eng. J. 232 (2013) 519–526.
[51] W. DiGuiseppi, C. Whitesides, T.K.G. Mohr, In Situ and on-site bioremediation, in: Proceedings of the 9th International In Situ Bioremediation Symposium Paper M-05, 7–10 May 2007, Baltimore, 2007.
[52] V. Augugliaro, V. Loddo, G. Marci, L. Palmisano, M. Schiavello, Chem. Biochem. Eng. Q. 9 (1995) 133–139.
[53] A.L. Linsebigler, G.Q. Lu, J.T. Yates, Chem. Rev. 95 (1995) 735–758.
[54] H. Barndõk, D. Hermosilla, L. Cortijo, C. Negro, A. Blanco, J. Adv. Oxid. Technol. 15 (2012) 125–132.
[55] N. Merayo, D. Hermosilla, L. Cortijo, Á. Blanco, J. Hazard. Mater. 268 (2014) 102–109.
[56] H.-S. Kim, B.-H. Kwon, S.-J. Yoa, I.-K. Kim, J. Chem. Eng. Jpn. 41 (2008) 829–835.
[57] H. Barndõk, L. Cortijo, D. Hermosilla, C. Negro, A. Blanco, J. Hazard. Mater. 280 (2014) 340–347.
[58] G.V. Buxton, C.L. Greenstock, W.P. Helman, A.B. Ross, J. Phys. Chem. Ref. Data 17 (1988) 513–886.

Update

Applied Catalysis B: Environmental
Volume 196, Issue , 5 November 2016, Page 232

DOI: https://doi.org/10.1016/j.apcatb.2016.05.062

Applied Catalysis B: Environmental 196 (2016) 232

Contents lists available at ScienceDirect

Applied Catalysis B: Environmental

journal homepage: www.elsevier.com/locate/apcatb

Corrigendum

Corrigendum to "Degradation of 1,4-dioxane from industrial wastewater by solar photocatalysis using immobilized NF-TiO_2 composite with monodisperse TiO_2 nanoparticles" [Appl. Catal. B: Environ. 180 (2016) 44–52]

Helen Barndõk[a], Daphne Hermosilla[a,*], Changseok Han[b], Dionysios D. Dionysiou[b], Carlos Negro[a], Ángeles Blanco[a]

[a] Department of Chemical Engineering, Universidad Complutense de Madrid, Avda. Complutense, s/n, 28040 Madrid, Spain
[b] Environmental Engineering and Science Program, Department of Biomedical, Chemical and Environmental Engineering (DBCEE), University of Cincinnati, Cincinnati, OH, USA

The authors regret to inform that, in the Acknowledgements section, the grant agreement number for the E4WATER project should read 280756 instead of 608490.

Acknowledgements

The research leading to these results has received funding from the European Union's Seventh Framework Programme (FP7/2007-2013) under the grant agreement no. 280756, E4WATER project.

Author would like to apologize for the inconvenience caused.

DOI of original article: http://dx.doi.org/10.1016/j.apcatb.2015.06.015.
* Corresponding author.
E-mail address: dhermosilla@quim.ucm.es (D. Hermosilla).

http://dx.doi.org/10.1016/j.apcatb.2016.05.062